

An Updated Estimate of Salinity for the Atlantic Ocean Sector Using Temperature–Salinity Relationships

MARLOS GOES AND JONATHAN CHRISTOPHERSEN

Cooperative Institute for Marine and Atmospheric Studies, University of Miami, and NOAA/AOML/Physical Oceanography Division, Miami, Florida

SHENFU DONG, GUSTAVO GONI, AND MOLLY O. BARINGER

NOAA/AOML/Physical Oceanography Division, Miami, Florida

(Manuscript received 25 February 2018, in final form 20 June 2018)

ABSTRACT

Simultaneous temperature and salinity profile measurements are of extreme importance for research; operational oceanography; research and applications that compute content and transport of mass, heat, and freshwater in the ocean; and for determining water mass stratification and mixing rates. Historically, temperature profiles are much more abundant than simultaneous temperature and salinity profiles. Given the importance of concurrent temperature and salinity profiles, several methods have been developed to derive salinity solely based on temperature profile observations, such as expendable bathythermograph (XBT) temperature measurements, for which concurrent salinity observations are typically not available. These empirical methods used to date contain uncertainties as a result of temporal changes in salinity and seasonality in the mixed layer, and are typically regionally based. In this study, a new methodology is proposed to infer salinity in the Atlantic Ocean from the water surface to 2000-m depth, which addresses the seasonality in the upper ocean and makes inferences about longer-term changes in salinity. Our results show that when seasonality is accounted for, the variance of the residuals is reduced in the upper 150 m of the ocean and the dynamic height errors are smaller than 4 cm in the whole study domain. The sensitivity of the meridional heat and freshwater transport to different empirical methods of salinity estimation is studied using the high-density XBT transect across 34.5°S in the South Atlantic Ocean. Results show that accurate salinity estimates are more important on the boundaries, suggesting that temperature–salinity compensation may be also important in those regions.

1. Introduction

Salinity is a key variable for determining density and steric height in the ocean; consequently, it affects the strength of ocean currents, the depth of the mixed layer, and the transport of mass, heat, salt, and nutrients across the globe. Ocean data assimilation relies on salinity observations and/or estimates for prediction of climate and weather patterns over marine and land areas. Without assimilation of salinity data, strong drift can occur in assimilation models as a result of poor knowledge of surface freshwater fluxes as well as limited understanding of mixing processes and the strength of the thermohaline circulation (Haines et al. 2006). A significant amount of the historical hydrographic profiles over the ocean (more than 4 million or 30%; www.nodc.noaa.gov) comes from

observations performed with mechanical and expendable bathythermographs (MBTs and XBTs, respectively), which provide only upper-ocean temperature measurements. These data contribute to long-term monitoring systems of global heat content, mixing, and volume and heat transport by the ocean currents (Goni et al. 2010; Cheng et al. 2016).

Historically, records of simultaneous temperature and salinity have predominantly come from conductivity–temperature–depth (CTD) and bottle station data. Although CTD profile data have high precision, the required ship time and personnel costs prohibit widespread use. Since 2004, autonomous Argo profiling floats provide nearly global measurements with more than 100 000 temperature–salinity profiles per year. These observations have greatly improved our knowledge of ocean water properties in the top 2000 m of the global ocean, and the assimilation of salinity profiles plays a significant

Corresponding author: Marlos Goes, marlos.goes@noaa.gov

DOI: 10.1175/JTECH-D-18-0029.1

© 2018 American Meteorological Society. For information regarding reuse of this content and general copyright information, consult the [AMS Copyright Policy](http://ams.org/PUBSRReuseLicenses) (www.ametsoc.org/PUBSRReuseLicenses).

role in improving ocean state estimation products and the skill of ocean forecast systems (i.e., [Smith and Haines 2009](#); [Huang et al. 2008](#); [Chang et al. 2011a,b](#)). Even after the spinup of the Argo system, XBT observations represent a very large subset of global upper-ocean temperature profile data, including more than 330 000 profiles in the Atlantic Ocean since 1990 (www.nodc.noaa.gov), and are still the most cost-effective platform to provide temperature data along fixed transects that can be used to

- 1) resolve and monitor variability of boundary currents,
- 2) estimate surface and subsurface current velocities and transports while resolving mesoscale features, and
- 3) study the variability of upper-ocean temperature (e.g., [Goes et al. 2013](#); [Domingues et al. 2014](#); [Lima et al. 2016](#)).

Since MBTs and XBTs measure only temperature profiles, it is necessary to infer their corresponding salinity profiles in order to estimate the haline contribution to the density and stratification of the ocean. Early studies (e.g., [Sverdrup et al. 1942](#)) considered the temperature–salinity (T – S) relationship as a conservative estimate in the ocean that allowed the definition of water masses by their T – S properties. [Stommel \(1947\)](#) highlighted the use of the mean T – S relationship to estimate salinity for dynamic height computation, a methodology that allowed the investigation of geostrophic ocean currents and volume transports when only temperature profiles are available. At higher latitudes, however, the T – S relationship may not be sufficiently conservative to be used for salinity estimations, and the salinity dependence with depth produces more reliable estimates of dynamic height (e.g., [Emery and O'Brien 1978](#); [Emery and Dewar 1982](#)).

Posteriorly, several more sophisticated methods, based on local regression techniques (e.g., [Hansen and Thacker 1999](#); [Thacker 2007](#); [Ballabrera-Poy et al. 2009](#)), empirical orthogonal functions (e.g., [Carnes et al. 1994](#); [Maes and Behringer 2000](#); [Chang et al. 2011a](#)), or high-order polynomials (e.g., [Marrero-Díaz et al. 2006](#); [Fox et al. 2002](#); [van Caspel et al. 2010](#)), have been developed to generate synthetic salinity profiles, from which many applied these techniques to infer water mass properties regionally (e.g., [Reseghetti 2007](#)). [Thacker \(2007\)](#) proposed a relatively simple and efficient scheme that relates salinity to the temperature squared at fixed depths, which has been widely used in studies of ocean currents, meridional overturning circulation (MOC), and meridional heat and freshwater transports (MHT and FWT, respectively) in the South Atlantic Ocean using XBT and satellite altimetry-derived temperature profiles (e.g., [Baringer and Garzoli 2007](#); [Dong et al. 2009, 2011](#); [Garzoli et al. 2013](#)).

Given the substantial increase over the past decade of salinity measurements from Argo profiling floats globally, and from underwater gliders and pinnipeds regionally, it is appropriate to update earlier methodologies by taking

advantage of improved global and regional coverage by adding more recent data. Here, we build upon previous studies by (i) including additional data, (ii) expanding the coverage of synthetic salinity estimates from regional to the whole Atlantic basin, and (iii) allowing the temporal variability of salinity by resolving seasonality and making inferences about interannual to decadal variability of salinity in the Atlantic Ocean.

This manuscript is structured as follows. [Section 2](#) describes the dataset used to construct the empirical relationships to estimate salinity from temperature profile data, and provides a description of the validation datasets, which includes the data used in the case study. [Section 2](#) also describes the four methodologies used that will be compared throughout the manuscript. [Section 3](#) compares the synthetic salinity and dynamic heights computed using the four methodologies, and shows the importance of including seasonal information to predict salinity near the surface. A case study for the MHT/FWT in the South Atlantic using the four methodologies is also given in [section 3](#). [Section 4](#) features the discussions and conclusions, as well as provides recommendations for future work.

2. Data and methodology

a. Data

The synthetic methodologies tested in this study rely on the use of in situ T and S profile measurements. Two main data sources are used as the trial population for a multivariate regression calibration. The first consists of historical simultaneous temperature and salinity profiles from the Coriolis Ocean Dataset for Reanalysis (CORA, version 3.4; [Cabanès et al. 2013](#)), which includes data from CTD, expendable CTD (XCTD), moorings, pinnipeds (mammals), underwater gliders, and Argo floats from 1990 to 2011. The CORA data used are from the World Meteorological Organization (WMO) instrument numbers 830 and 700–751 (http://www.wmo.int/pages/prog/www/WMOCodes/WMO306_v12/LatestVERSION/WMO306_v12_CommonTable_en.pdf), and are flagged as good data (quality control flags 1 and 2), according to the WMO standard. Additionally, data from the global Argo float dataset available from 2012 to 2015 are also included in a trial population. The Argo data are from the National Oceanic and Atmospheric Administration (NOAA) global Argo repository (<https://www.nodc.noaa.gov/argo/>), where only the delayed mode data are used, and from the floats distributed within the Atlantic domain.

In this work, all the data are vertically interpolated to standard depth levels in order to constrain all profiles to the same vertical axis and to reduce the occasional vertical gap in profile data. To accomplish this, a locally

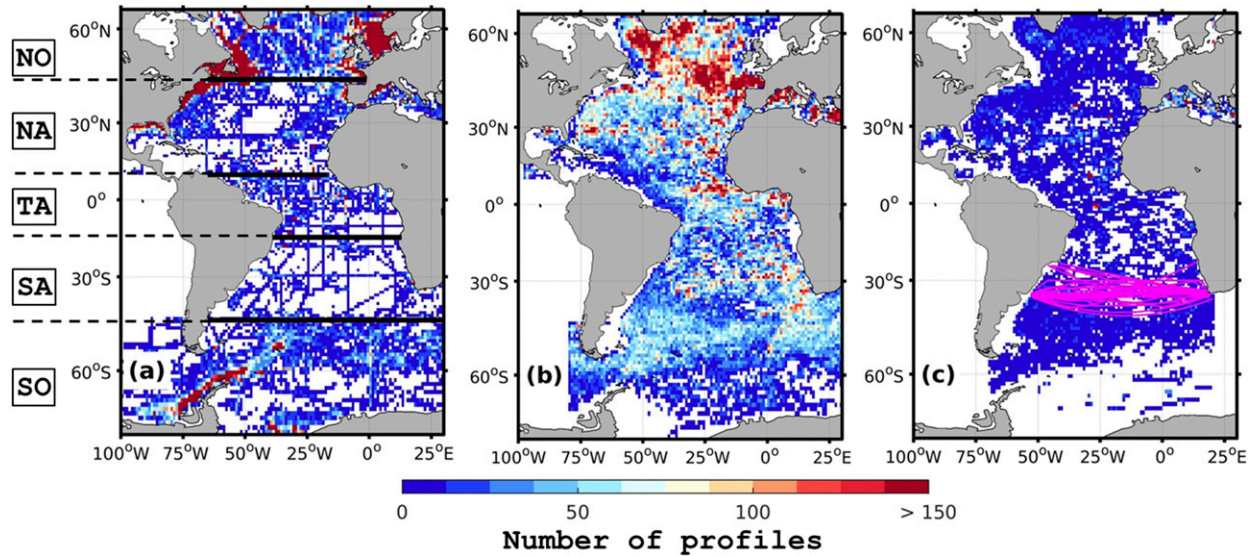


FIG. 1. Distribution of the number of profiles per degree squared used as a trial population in the statistical method subdivided into (a) CORA dataset (1990–2015; excluding Argo) and (b) Argo-only data (1998–2015). (c) Profiles per degree square for the Argo 2016 validation dataset overlaid by the locations of the AX18 transects (magenta lines). The domain comprises the Atlantic Ocean between 70°S and 65°N, and the black lines in (a) are the locations of the five regional basins analyzed.

weighted scatterplot smoothing (LOWESS) filter is applied with windows of 30 and 150 m, which is a compromise between low and high variability in the profiles. A total of 85 standard levels are used from 7.5 to 2000 m, using a spacing of 10 m in the top 300 m, and 20 m farther down. The study domain is the entire Atlantic Ocean basin with portions of the Arctic Ocean and the Southern Ocean, comprising the latitudes between 70°S and 65°N and longitudes between 100°W and 30°E. A total of approximately 1 000 000 profiles are used as input in the regression. It is noteworthy that the number of profiles used in this study is larger than in any other similar study (Korotenko 2007; Thacker 2008; Ballabrera-Poy et al. 2009).

The distribution of the trial profile population across the Atlantic domain used in the calibration is shown in Fig. 1, divided for illustration purposes into non-Argo CORA and Argo-only datasets. The non-Argo CORA data generally follow cruise transects and show a high density of more than 100 profiles per degree square near the boundaries, particularly along the Antarctic Peninsula and north of 30°N (Fig. 1a). The distribution of Argo data is much more homogeneous over the study domain. The North Atlantic, especially north of 30°N, is where the density of hydrographic profiles is the highest, frequently more than 100 profiles analyzed per degree square for both the CORA and Argo datasets. Regions with the lowest density of profiles are located in the Caribbean Sea, the southeastern tropical Atlantic, and the Southern Ocean, with often fewer

than 30 profiles per degree square. Near the coastal boundaries and in shallow marginal seas such as the North Sea, between Great Britain and Scandinavia, Argo distribution is very low or inexistent, although CORA data compensate for some of this lack of Argo data. The distribution of data per year shows a strong increase in the number of profiles after 2000 in all basins. Before 2000, the Southern Ocean and the South Atlantic basin had fewer than 1000 profiles per year.

The validation dataset used in this work is the Argo salinity and temperature data from 2016. These data are excluded during calibration and are therefore independent. A total of approximately 57 000 profiles are withheld for validation across the whole study domain. We introduce a case study using the AX18 XBT transect data. The AX18 transect is bounded by South Africa and South America, and is aimed at monitoring the MOC in the South Atlantic along the nominal of 34.5°S (Baringer and Garzoli 2007). As part of the AX18 transect, temperature profiles are obtained quarterly in the top 850 m of the ocean, with a nominal longitudinal sampling of 25 km. A total of 45 realizations of this XBT transect are used, from which the MOC, MHT, and FWT are estimated.

b. Methods

In this study, we use a multivariate linear regression method to estimate salinity from observed temperature,

location, and time of observations. In this regression, we assume that the outcome $S = S(\theta)$ is a function of several predictors θ . The predictors typically available in profiles such as the XBT data are T , depth z , month of the year (mo), year (yr), latitude (lat), and longitude (lon). Other predictors could be used as well, such as sea surface height (Guinehut et al. 2012; Goes et al. 2013; Chang et al. 2011a), sea surface salinity (Hansen and Thacker 1999; Ballabrera-Poy et al. 2009; Yang et al. 2015), and surface freshwater fluxes [runoff, and evaporation minus precipitation ($E - P$)]. However, their use would impose the need for additional datasets (e.g., satellite data), which may not be available at the time of prediction, and therefore will not be included in this study as predictors. The first, simple step should be to use annual, seasonal, or monthly climatologies of T - S relationships with depth. These are the ones explored here.

Formally, the vector \mathbf{A} of p parameters, $\mathbf{A} = (a_1, a_2, \dots, a_p)$, is estimated at each depth and horizontal location according to

$$\mathbf{Y} = \mathbf{A}\mathbf{X}, \quad (1)$$

where $\mathbf{Y}_{z \times n}$ is the vector of n centered salinity values,

$$\mathbf{Y} = [S - \langle S(z) \rangle], \quad (2)$$

where $\langle S(z) \rangle$ is the horizontally weighted mean of the n profiles in each bin. The matrix $\mathbf{X}_{p \times n}$ is the predictor matrix, composed of p rows and n columns.

Here, we compare four different empirically derived methods to estimate salinity from temperature profiles. Two of these are T - S lookup-based methods (1 and 2), which are derived using information of the mean salinity and/or temperature only, and the other two methods (3 and 4) are based on local regressions at each depth with varying numbers of parameters in the matrix \mathbf{X} used in the regression. The methods are described as follows:

- 1) TSMEAN: This method was first developed by Stommel (1947), in which for each bin $S = \langle S(T) \rangle$. Therefore, salinity is estimated from the local mean T - S curve by matching $\langle T(z) \rangle$ profiles using a linear interpolation on the T space. This method conserves the T - S curve but suffers from uncertainties resulting from interpolation biases when water masses are too homogeneous (Stommel 1947).
- 2) SMEAN: In this method only the information of the mean $\langle S(z) \rangle$ profile is used to estimate the salinity at a particular location. This method is similar to the methodology used by Emery and Dewar (1982), which assumes that in regions where the T - S relationships

feature inflection points or small variability over the majority of the water column, $S = \langle S(z) \rangle$ is more reliable than the TSMEAN method. This is achieved by solving Eq. (1) for

$$\mathbf{Y} = 0. \quad (3)$$

- 3) RDIST: This method was developed by Thacker (2008), which assumes that salinity at a particular depth can be estimated using a linear combination of temperature, temperature squared, and the distance (latitude and longitude) to the center of the grid:

$$\mathbf{X} = [T, T^2, \text{lon}, \text{lat}]. \quad (4)$$

- 4) RSEAS: The method presented in this study is similar to RDIST, and also introduces seasonality to the regression. Seasonality is accounted for by replacing the distance terms in Eq. (4) with the annual and semiannual harmonics in the regression. Including seasonality in the regression by fitting the annual and semiannual harmonics adds four additional terms, and reduces the potential skewness of the residuals when there are nonuniform seasonal distributions of data in the regions (Ridgway et al. 2002; Machín et al. 2008). Therefore,

$$\mathbf{X} = \left[T, T^2, \cos\left(2\pi \frac{\text{mo}}{12}\right), \sin\left(2\pi \frac{\text{mo}}{12}\right), \cos\left(4\pi \frac{\text{mo}}{12}\right), \sin\left(4\pi \frac{\text{mo}}{12}\right) \right]. \quad (5)$$

In Eq. (5), the variance of the seasonal cycle can be assessed using

$$\text{Var} \sim N(a_3^2 + a_4^2 + a_5^2 + a_6^2) / [2(N - 1)], \quad (6)$$

where N is the number of observations, and a_3 - a_6 are the coefficients associated with the annual and semiannual harmonics in Eq. (5).

Similar to the salinity, the predictors on the right-hand side of Eqs. (3)-(5) are all individually centered (zero mean). For this, all methods use the same mean salinity profile $\langle S(z) \rangle$ estimated in SMEAN, and RSEAS and RDIST use the same temperature mean profile $\langle T(z) \rangle$ as estimated in TSMEAN. Regardless of the methodology applied, each regression is evaluated at the center of each $1^\circ \times 1^\circ$ bin. A minimum of 150 profiles are considered in each bin. Although this criterion is not always met, it is chosen in the attempt to reduce the mesoscale variability in the mean. If the number of profiles within a bin is smaller than 150, we include the nearby data, following a 0.2° increase in the search radius up to a maximum area of 4° or 150 profiles, whichever

is smaller. Fitting the data with overlapping regions is advantageous for adding more data to the fitting, as well as for guaranteeing smooth variations across cells (Thacker 2008). In the regression-based methods (RDIST and RSEAS), one regression is performed at each depth level; therefore, depth is treated as a categorical (qualitative) variable. Surface salinity is calculated as an extrapolation to the first estimated level (7.5 m). For all depths, data weights are defined as a function of latitude and longitude assuming a spatial double exponential autocorrelation function (e.g., Goes et al. 2010) with an isotropic e -folding scale of 2° from the center of each cell and a variance of 1 psu^2 .

3. Results

Here we present results in the spatial domain defined between 70°S and 65°N in the Atlantic Ocean. We first present the regional aspects shared by the statistical methods, with an emphasis on the RDIST and RSEAS methods, which are the methods based on a multivariate regression, and the evolution of the residuals output directly from the regression. Next, we present results using the validation dataset, where we show the effects of all empirical salinity methodologies on the salinity profiles and dynamic height, followed by the time evolution of the residuals, where half of the historical data are selected as the trial dataset and the other half of the data are used for validation. Finally, we show results using data from the AX18 XBT transect along 34.5°S , and analyze the impact of the different estimates of salinity on the MOC and MHT computations using these data.

a. Regional and temporal features of the regression-based methodologies

REGIONAL ASPECTS

Here we describe the regional features of the methodologies presented in the previous section. The distance Λ (Fig. 2a) corresponds to the length of the squared area taken into account for the weighted regression in each 1° grid cell. The coefficient Λ is therefore dependent on the data availability in each region. In the North Atlantic (NA) and northern ocean (NO), as a result of the dense data coverage over time, Λ is close to its minimum value of 1° . There is one exception, the Caribbean Sea, where data are scarcer. Because of the shallow bathymetry over most of the region, Argo floats are not deployed in the Caribbean, as they cannot sample waters shallower than 2000 m. The tropical Atlantic (TA) and South Atlantic (SA) are relatively well covered, especially after Argo, with exceptions near the

boundaries, shallow continental shelves off southeastern South America, and in the center of the subtropical gyre, where there is little residence time for the Argo floats. It is worthy of notice that the data coverage may change significantly for other databases and other versions of CORA. The Southern Ocean (SO) is the region with least data coverage, and Λ values are often above 2.5° wide. The distribution of the root-mean-square (RMS) of the salinity residuals from the RSEAS method (Fig. 2b) shows that the RMS error is in general below 0.05 psu. However, the regions with strong currents and eddy activities, such as the Brazil–Malvinas confluence, the North Brazil Current, the Gulf Stream, and the Nordic seas, experience larger errors, up to 0.3 psu. These regions are characterized by high variance of salinity as a result of strong eddy activity, seasonality (Fig. 2c), and potentially longer-term variability. The ratio between the RMS errors from RSEAS and RDIST (Fig. 2d) is lower than 1 in most of the domain, suggesting that the RSEAS gives better salinity estimates. As expected, the RSEAS method has higher gain in the regions with stronger seasonality in salinity (Fig. 2c). Regions of lower data density (Fig. 2a), such as in the southeastern South American continental shelf or SO are the ones where the RDIST method improves over the RSEAS method. This is also expected, since the RSEAS method has two additional estimated parameters and therefore a reduced number of degrees of freedom.

b. Mean differences

1) SALINITY

The Argo data from 2016 over the study domain are used to estimate the error of salinity inferred by the four methods in each of the five regions: NO, NA, TA, SA, and SO. For easy visualization, one sample is given to demonstrate the performance of each method in all five regions, in which a typical salinity profile and its respective T – S curve from an Argo profile are compared to the same profile with salinity replaced by its estimates (Fig. 3). In general, all methods capture the structure of salinity profiles and T – S curves in all regions. A mean bias of ~ 0.1 psu is evident in the T – S curve of the SO profile, and all the other profiles show a good agreement over depth. The SMEAN method (blue in Fig. 3) shows large differences (>0.8 psu) in the T – S diagrams, and also larger differences relative to Argo than the other methods in the tropical and subtropical regions. In the SO, however, the SMEAN method agrees better with the other methods. The TSMEAN method shows better agreement with Argo than the SMEAN method in the tropical–subtropical regions. The TSMEAN method (green in Fig. 3) generally fails within the intermediate

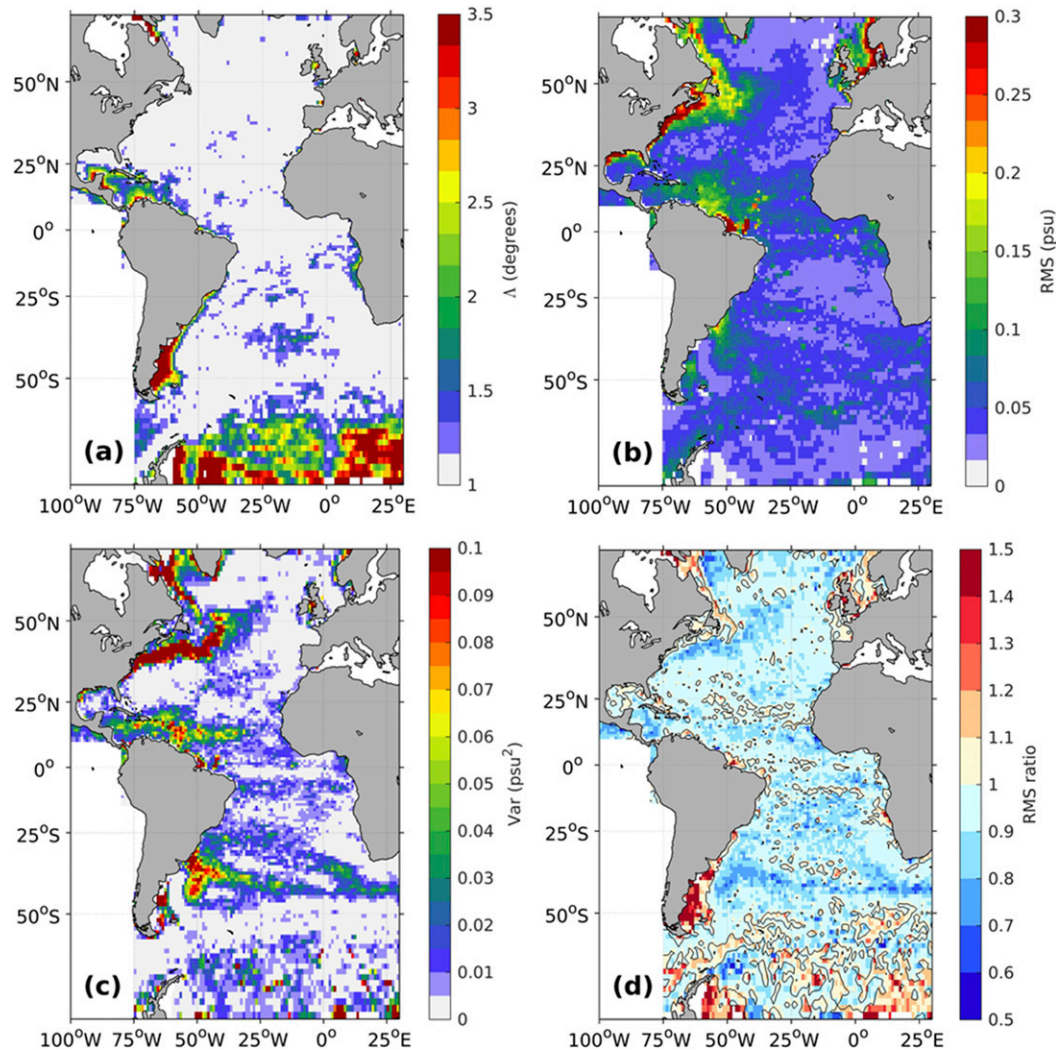


FIG. 2. (a) Box size (Δ , $^{\circ}$) that encompasses the profiles used in the regression, (b) RMS error (psu) between the estimated and original salinity using only the profiles within 1° distance from the center of each box, (c) variance of the harmonics in the top 100 m calculated using the RSEAS method, and (d) RMS error ratio (RSEAS/RDIST).

waters, between 800 and 1100 m in the TA and SA regions, where the temperature is flat in the T - S diagrams, and also in the SO between 300 and 700 m. The RDIST (red in Fig. 3) and RSEAS (orange in Fig. 3) methods agree better with the Argo observations than the other two methods, and are very similar, almost indistinguishable, below 400 m in all cases. This is where the T and T^2 terms dominate the multivariate regression, and hence this agreement is not surprising. In contrast, the methods tend to diverge more in the upper 150 m, with RSEAS exhibiting the best agreement with Argo, which can be seen clearly in the NO region.

To assess the accuracy of each method to infer salinity at different depths, we examine the 90% confidence interval (CI) of salinity residual distributions, which is

defined as the average between the 5th and 95th percentiles of the residual probability distributions of the profiles in each region and depth. Figure 4 shows in the upper panels the 90% CI of all regions, averaged within four layers bounded by the 0-, 200-, 800-, 1200-, and 2000-m depths. All basins exhibit a similar behavior, that is, with wider distributions in the top few hundred meters of the ocean and converging to much narrower distributions below the thermocline. Larger errors in the upper ocean are expected, as this is the region where the T - S relationship breaks down as a result of strong surface fluxes, and eddy and mixing activities. The mean salinity (SMEAN) only cannot represent the regions with high T - S variability, such as the SA and NA, and the salinity errors have a much wider distribution at

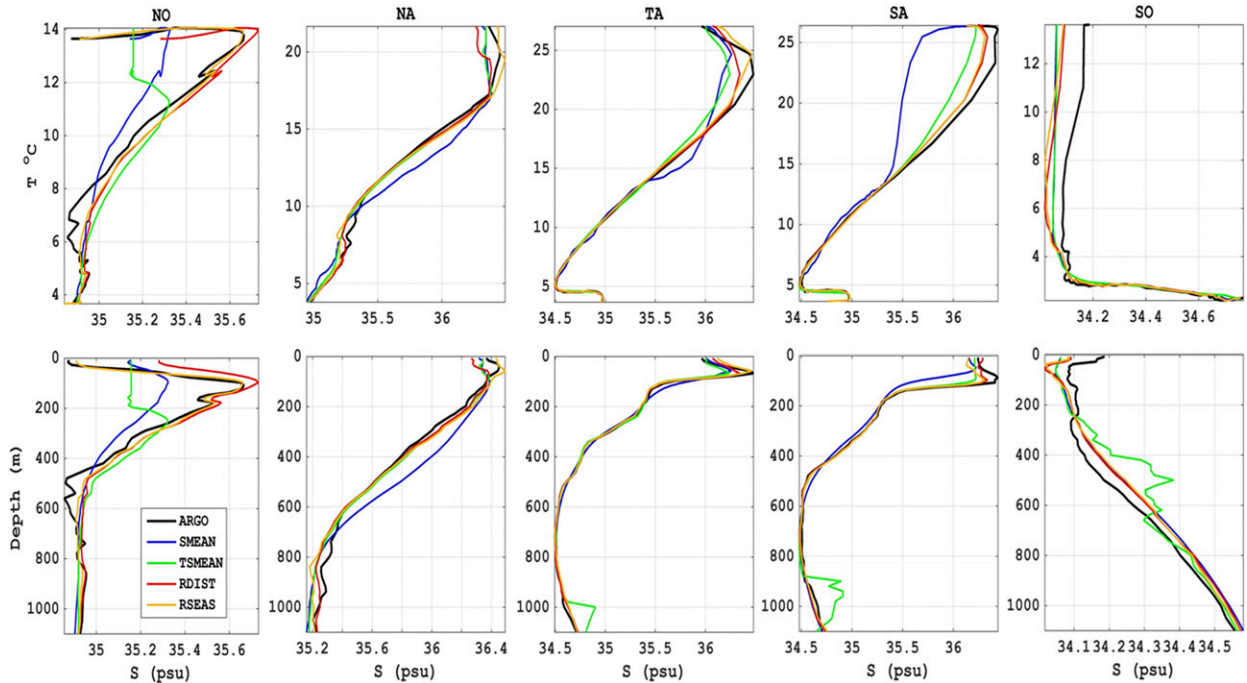


FIG. 3. Comparison of (top) T - S diagrams and (bottom) salinity profiles from Argo 2016 (black) with the estimates from the SMEAN (blue), TSMEAN (green), RDIST (red), and RSEAS (orange) methodologies. Panels are divided sideways for each basin: (left to right) NO, NA, TA, SA, and SO.

lower depths. The TSMEAN method has a fairly similar behavior to the SMEAN method in the NA and NO regions, and performs better at central depths where there are strong linear T - S relationships. However, in the TA, SA, and NO regions, this method cannot represent the regions where the Antarctic Intermediate Water is located—that is, depths between 800 and 1200 m—because of the inversion of the T - S curve that is characteristic of this water mass (see Fig. 3). In the SO, because of the strongly homogeneous temperature profile, the TSMEAN method has large errors (90% CI ≥ 0.3 psu) throughout the whole water column. The RDIST method reduces considerably the errors at depth relative to the TSMEAN and SMEAN methods, and the 90% CI is below 0.3 psu in the upper 200 m and less than 0.1 psu below 200 m in all five regions. The RSEAS method performance is very similar to that of RDIST, but it shows a slight reduction (~ 0.05 psu) in the residual spread near the surface. The implications of these errors to the dynamic height estimations are analyzed next.

2) DYNAMIC HEIGHT

The dynamic height is the most appropriate parameter to infer the influence of salinity on dynamical changes in the ocean, since it is closely related to a

streamfunction to estimate oceanic steric flows. The residual distributions of the surface dynamic height relative to 500 m (DH_{500}) are calculated for all five subregions of the study domain (Fig. 4, lower panels). These residuals are the differences of dynamic height calculated using the Argo 2016 T - S data against the dynamic height derived from the Argo temperature profile and salinity produced by the four T - S lookup methods.

The SMEAN method presents higher DH_{500} residuals in all subregions relative to the three other methods, except for the TSMEAN method in the SO, since the TSMEAN method shows strong caveats in regions where temperature is homogeneous (i.e., Fig. 3). The 90% CI of the residuals for the SMEAN method is [4.4, 7.7, 3.8, 10.7, and 6.7] dyn cm over the [SO, SA, TA, NA, and NO] regions, respectively, compared to the 90% CI values of [10.9, 4.5, 2.5, 9.5, 5.2] dyn cm for the TSMEAN method. The 90% CI of the residual values are for RDIST [3.1, 3.1, 2.3, 4.5, 3.8] dyn cm and for RSEAS [3.4, 2.9, 2.2, 4.5, 3.4]; therefore, both methods show maximum dynamic height (relative to 500 m) errors of less than 4.5 dyn cm, and their errors are in general 30% smaller than the SMEAN method. Apart from the SO region, where the RDIST method outperforms the RSEAS method (3.1 against 3.4 dyn cm), all other basins

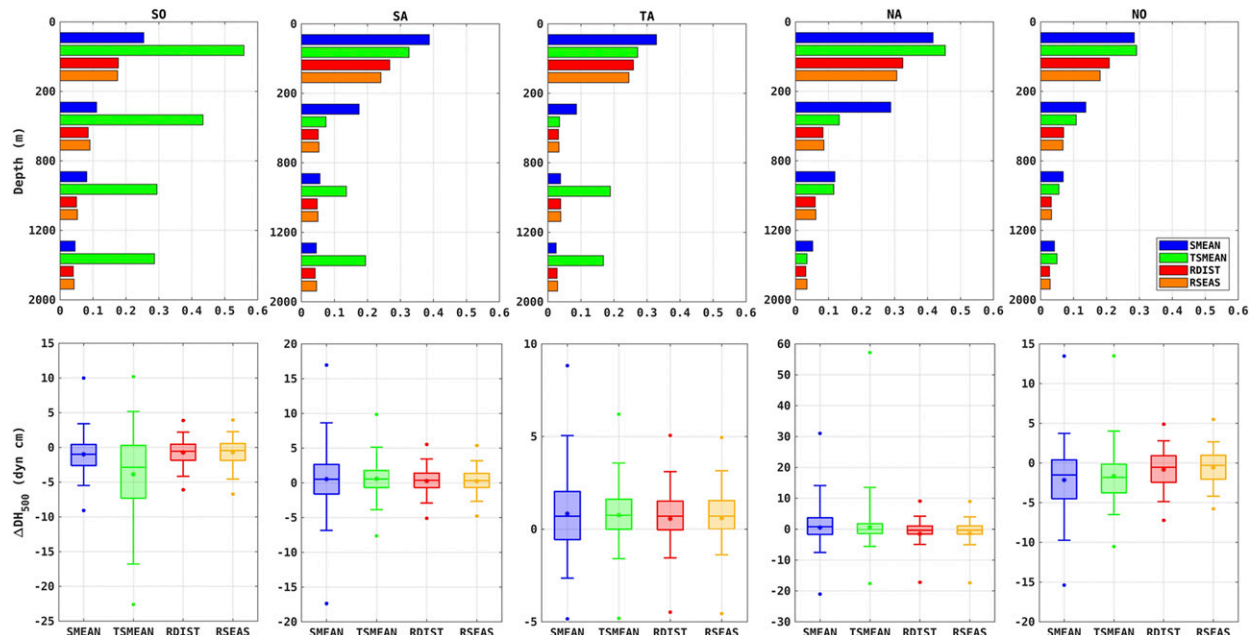


FIG. 4. (top) Bar plots of 90% CI of the residual differences (psu) averaged within depth ranges 0–200, 200–800, 800–1200, and 1200–2000 m applied to the Argo 2016 salinity profiles using each of the four salinity estimation methods. (bottom) Distribution of surface dynamic height differences (dyn cm) referenced to 500 m using the Argo 2016 profile data. Box represents the 25th and 75th percentiles, the whiskers represent the 5th and 95th percentiles, and dots indicate the mean and the full width of the distributions. Each panel is for one subbasin (from left to right: SO, SA, TA, NA, and NO), and the box-and-whisker colors are associated with the SMEAN (blue), TSMEAN (green), RDIST (red), and RSEAS (yellow) methods.

show a slight reduction in DH_{500} errors using the RSEAS method relative to the RDIST method.

c. Time evolution of residuals

To investigate the time evolution of the salinity residuals, we compare the basin-averaged monthly salinity residuals of the four methods within all five basins (Fig. 5). To perform this analysis, we recomputed the methods using only half of the trial population from 1990 to 2015 (Fig. 1) and used the other half for verification. The significance of these residuals is of course dependent on the number of profiles used every month. To reduce coverage biases, this comparison is shown only for the period of 1999–2015. Several regionally specific features can be captured in this comparison. In the SO (Fig. 5a), the TSMEAN method produces strong positive salinity bias $\Delta S > 0.2$ in the top 400 m of the ocean as a result of strongly mixed waters in the upper ocean. SMEAN and RDIST produce similar results, and the residuals show strong seasonality in the top 200 m, where the residuals alternate from positive to negative within a year, superimposed onto a smaller interannual residual variability, which is also observed in RSEAS. In the SO and SA, the RSEAS method reduces significantly the seasonality of the residuals relative to RDIST because it accounts for the first two harmonics [Eq. (5)].

In the SA, the TSMEAN method improves considerably over the SO, and the amplitude of its averaged salinity residuals is generally $|\Delta S| < 0.1$. Some seasonality of the residuals is observed in the SMEAN method in SA in the top 150 m (Fig. 3b), which is surprisingly enhanced in the RDIST method. This residual seasonality is clearly seen when comparing the averaged 150-m residual salinity time series of RDIST against RSEAS in the top panel of Fig. 5b. In the TA (Fig. 5c), there is little seasonality and modest interannual variability in the residuals in the RDIST, RSEAS, and SMEAN methods, and the highest residual variability is concentrated in the top 100 m. The RDIST and RSEAS methods perform comparably well in the TA region, although the magnitude salinity residuals in RSEAS is typically slightly smaller (< 0.02 psu) than in RDIST. In NA and NO (Figs. 5d,e, respectively), there is strong interannual variability that is coherent between the two basins, with an approximately 5-yr cycle until 2010 and a more stable behavior after 2010. The causes of this basinwide variability north of 15°N may be related to the modulation of the $E - P$ by large-scale phenomena, such as the North Atlantic Oscillation (e.g., Reverdin et al. 2002). In NA and NO, the salinity residuals from TSMEAN show strong freshening in the top 100 m and salinification below it, characterizing some depth compensation of

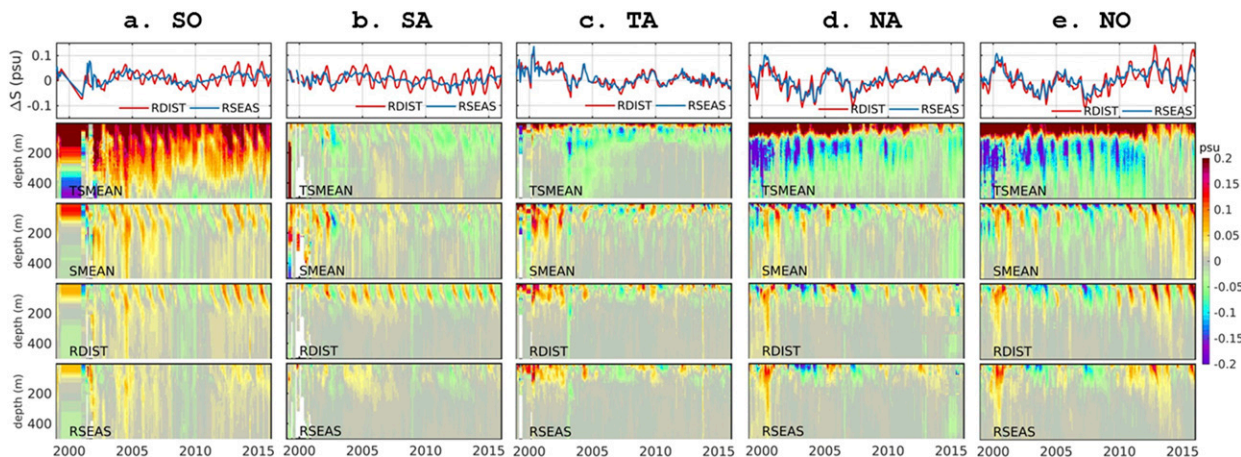


FIG. 5. Time evolution of salinity residuals (psu) for the different methods averaged over each basin in the Atlantic sector from 1999 to 2015. (top) Respective time series of averaged residuals in the top 150 m for the RSEAS (blue) and RDIST (red) methods. The contour panels are the monthly averaged profiles in each basin for the (from top to bottom) TSMEAN, SMEAN, RDIST, and RSEAS methods.

the residuals. Some seasonality of the residuals in SMEAN and RDIST is observed in the NA and to a larger extent in the NO regions, where the amplitude of the seasonal variability is comparable to the interannual variability.

The RSEAS exhibits far less seasonal variability in the NA and NO regions and, thus, it outperforms the RDIST method. This decrease in seasonal variability of the residuals is further illustrated by taking the autocorrelation function (ACF) of the residual time series averaged over the NO (Fig. 6). The ACF decay of approximately 30 months in the RSEAS method (Fig. 6c) is due to the large-scale interannual variability in the region. The RDIST method is still strongly affected by the seasonality of the residuals time series (Fig. 6d), and its ACF is characterized by alternating peaks of about 12 months. Although not discussed here, the interannual variability of the RSEAS residuals can potentially be addressed as a low-order autoregressive model, as shown by the significant peaks in the partial ACF functions (Figs. 6e,f).

d. South Atlantic MHT and FWT

One important application of the salinity estimate methods is the computation of water mass, heat, and freshwater transport using XBT temperature profile data. Here we assess the sensitivity of the MHT and the FWT to the salinity in the upper 800 m estimated from the four methods introduced earlier. We use for this comparison data from the AX18 transect along the nominal latitude of 34.5°S in the South Atlantic. The MHT and FWT are estimated following the methodology of Dong et al. (2009; 2011) and Garzoli et al. (2013), in which the deep salinity and temperature are padded from the 1/4° World Ocean Atlas 2013 (WOA13) seasonal

climatology (Locarnini et al. 2013; Zweng et al. 2013). The cross-transect geostrophic velocities are estimated from dynamic height referenced to the $\sigma_2 = 37.09 \text{ kg m}^{-3}$ surface and corrected to allow a 0.04 m s^{-1} at the bottom along the western boundary. Previous studies have analyzed the impact of the methodological approximations and XBT measurement uncertainties on the calculation of the meridional overturning and meridional heat transports across the AX18 transect (Baringer and Garzoli 2007; Goes et al. 2015a,b). By simulating the AX18 observing system in a model, those studies suggested that the choice of the reference depth is the largest uncertainty in the methodology, and that XBT depth biases do not contribute significantly to MOC/MHT biases shorter than decadal time scales. Biases induced by salinity estimates from the T - S relationship and padding of climatology below XBT measurement depth are relatively small, contributing as much as 1 Sv ($1 \text{ Sv} \equiv 10^6 \text{ m}^3 \text{ s}^{-1}$) at seasonal time scales.

The RMS differences in salinity and cross-sectional velocities among the four methods are shown in Fig. 7. The salinity differences between RDIST and RSEAS are generally below 0.1 psu, mostly concentrated in the top 150 m. In the western boundary, west of 40°W, the two methods show greater differences, up to 0.2 psu. As shown in Fig. 2, this is a region of low data density along the shelf, but with strong seasonality in salinity potentially resulting from the high variability near the Brazil–Malvinas confluence zone (Fig. 2c). Therefore, in this region the RSEAS method performs particularly well (Fig. 2d). Derived velocity differences obtained using these methods (RDIST minus RSEAS) are small, typically below 0.03 m s^{-1} (Fig. 7d).

Salinity differences between the SMEAN and RSEAS methods (Fig. 7b) are much larger and widespread than

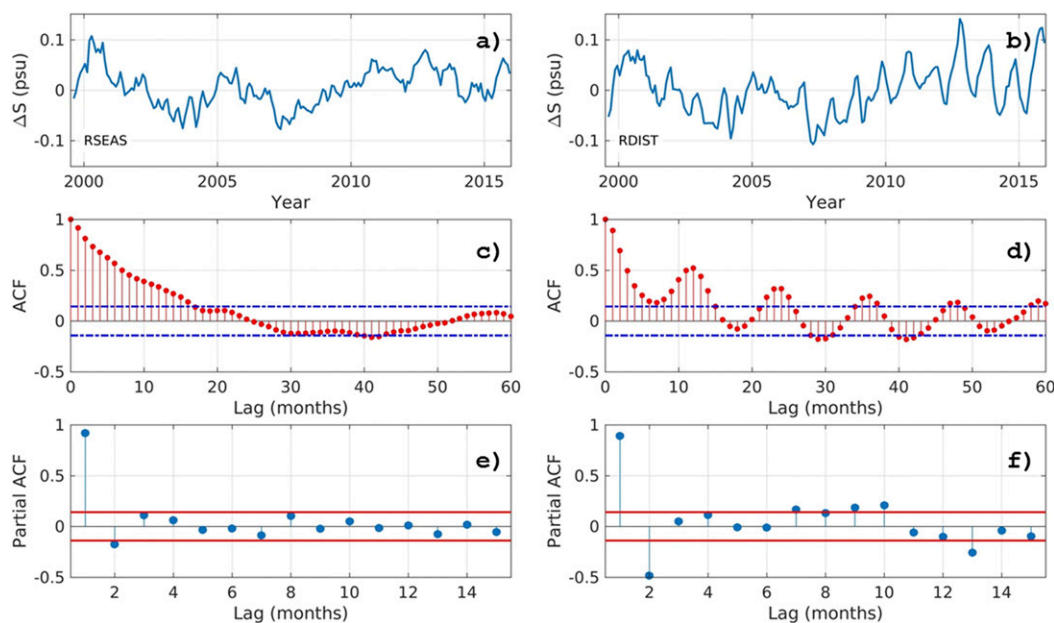


FIG. 6. (a),(b) Time series; (c),(d) autocorrelation function; and (e),(f) partial autocorrelation function from the time series of the residual salinity (estimate minus observation) averaged in the top 150 m over the northern ocean region. (left) RSEAS and (right) RDIST methods.

(RDIST minus RSEAS). SMEAN–RDIST salinity differences are very similar to Fig. 7b, thus not shown. The boundaries are again the region with the highest differences, exceeding 0.2 psu across the water column between 200 and 500 m at central water depth range (Fig. 7b). This depth range is where there is strong compensation between salinity and temperature, which are not captured by the SMEAN method. Derived velocity differences (SMEAN minus RSEAS) can reach 0.2 m s^{-1} in the top 300 m (Fig. 7e). The TSMEAN method (Figs. 7c,f) has a better representation of the water masses in this region than the SMEAN method. Salinity differences (TSMEAN minus RSEAS) are generally lower than 0.125 psu, increasing to 0.2 psu west of 40°W , which may suggest again, similar to the comparison with RDIST (Fig. 7a), that strong seasonality exists in the upper layer, particularly in the western boundary. The (TSMEAN minus RSEAS) velocity differences (Fig. 7f) reflect the same intensified upper-ocean variability.

The MHT and FWT time series from XBT transects with salinity derived from the four methods are shown in Fig. 8. Variations in the MOC (not shown), MHT, and FWT on both seasonal and interannual time scales are very similar, suggesting that the thermosteric contributions to dynamic height dominate their variability. FWT variability is opposite of MHT and MOC, since fresh-water is defined as $(S_0 - S)/S$, where S_0 is the mean salinity along the section (Garzoli et al. 2013). The mean strength of the MOC (not shown), MHT, and FWT

for the RDIST and RSEAS methods are $\sim 19.3 \pm 4 \text{ Sv}$, $0.51 \pm 0.2 \text{ PW}$, and $-0.33 \pm 0.3 \text{ Sv}$, respectively, similar to previous estimates that used a method similar to RDIST. These values are greater than the ones using the SMEAN method ($18.5 \pm 5 \text{ Sv}$, $0.41 \pm 0.4 \text{ PW}$, and $-0.26 \pm 0.4 \text{ Sv}$) and are slightly lower than the estimates using the TSMEAN method ($19.4 \pm 4 \text{ Sv}$, $0.53 \pm 0.2 \text{ PW}$, and $-0.36 \pm 0.3 \text{ Sv}$). Interestingly, the SMEAN method allows for a reversal of MHT (negative values), which is not seen in the other methods (Fig. 8a). The seasonal cycle of MHT (MOC) shows a semiannual pattern, with higher values during February–April and August–September, and lower values during June and October/November (Figs. 8c,d), which is similar to that of FWT (stronger in April/September). According to the numerical model analysis of Goes et al. (2015a), salinity errors derived from a T – S lookup table show seasonal behavior with RMS errors of $\pm 1 \text{ Sv}$. Similarly, we investigate the seasonality of the MHT and FWT residuals relative to RSEAS (Figs. 8e,f). The RDIST–RSEAS differences are small, typically lower than $\Delta\text{MHT} \sim 0.02 \text{ PW}$ and $\Delta\text{FWT} \sim 0.06 \text{ Sv}$, and with opposing phase to the seasonal cycle shown in Figs. 8c and 8d, suggesting that the seasonality not captured by the RDIST method (see Fig. 5b) has a small influence ($\sim 1\%$) in reducing the meridional transports.

The monthly mean MHT residuals of the SMEAN method are on order of magnitude higher than the ones from the other three methods, and are scaled by 10^{-1}

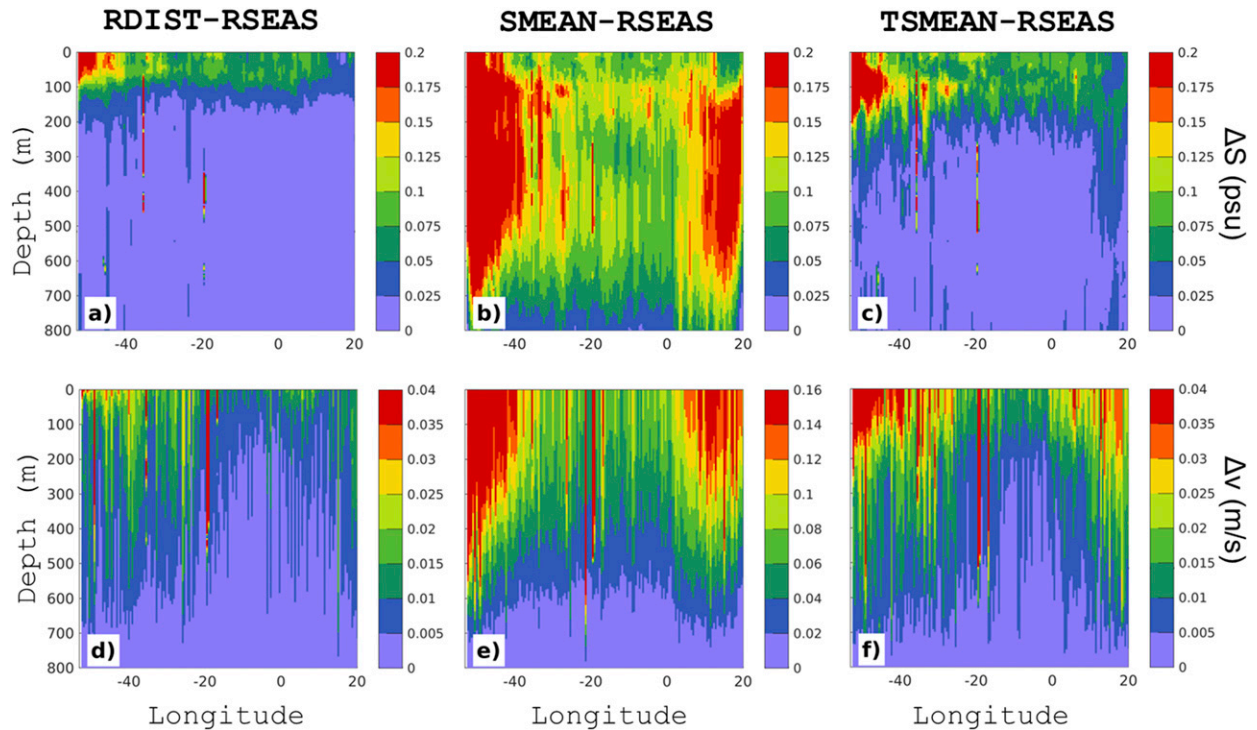


FIG. 7. RMS differences of (a)–(c) salinity and (d)–(f) velocity estimated in the top 800 m for the AX18 sections. The differences are calculated relative to RSEAS for the RDIST, TSMEAN, and SMEAN methods (labels above the top panels). Note that the SMEAN–RSEAS velocity differences shown in (e) display increased color bar range relative to (d) and (f).

in Fig. 8e. Particularly in the second half of the year (June–December), when MHT shows lower values, SMEAN underestimates the heat transport by up to 0.3 PW. As oppose to the RDIST method, the SMEAN method shows a strengthened seasonality in MHT and FWT across 34.5°S. This result corroborates with Fig. 7, in that temperature–salinity compensation occurs at this latitude, which tends to reduce the transport variability but is not captured using the SMEAN method.

4. Discussion and conclusions

The upper-ocean (<200 m) variability presents one of the greatest challenges in estimating salinity from temperature profiles. This is because the T – S relationships break at the surface as a result of strong mixing and surface fluxes. Here, we introduce a direct and self-contained methodology for the construction of salinity lookup tables from temperature profile data. A regression method is used to construct a relationship between salinity, temperature, depth, month, and geographical location. Seasonality is one potential contributor to the variance (and covariance) of the residuals in the upper ocean. We show that substituting the horizontal predictors using the seasonal information consistently improves the salinity

estimates in the top 150 m of the ocean. Seasonality is important in key regions of the ocean, including frontal systems, boundaries, and close to the equatorial region. Below 150 m, seasonality is less important, and the simple relationship of salinity with depth and temperature can provide a very good approximation.

Our results agree in part with early studies, which show that a mean T – S curve can capture most of the halosteric variability in the ocean. However, this relationship does not hold in regions of low stratification, high mixing, and where the T – S relationship is weak, such as the Antarctic Intermediate Water (AAIW) layers. In those regions, such as the Southern Ocean and depths below 1600 m, inferring salinity from a depth annual mean profile can be more efficient. However, in most locations and particularly in the upper ocean, the SMEAN method is the least effective to estimate salinity. One of the most important findings in this study reveals that the variations in the MHT and FWT in the South Atlantic on both seasonal and interannual time scales are very similar regardless of variations in salinity estimates, which may be indicative that the thermosteric contributions to dynamic height dominate the MHT and FWT variability. This result is important because it highlights the value of estimates produced using

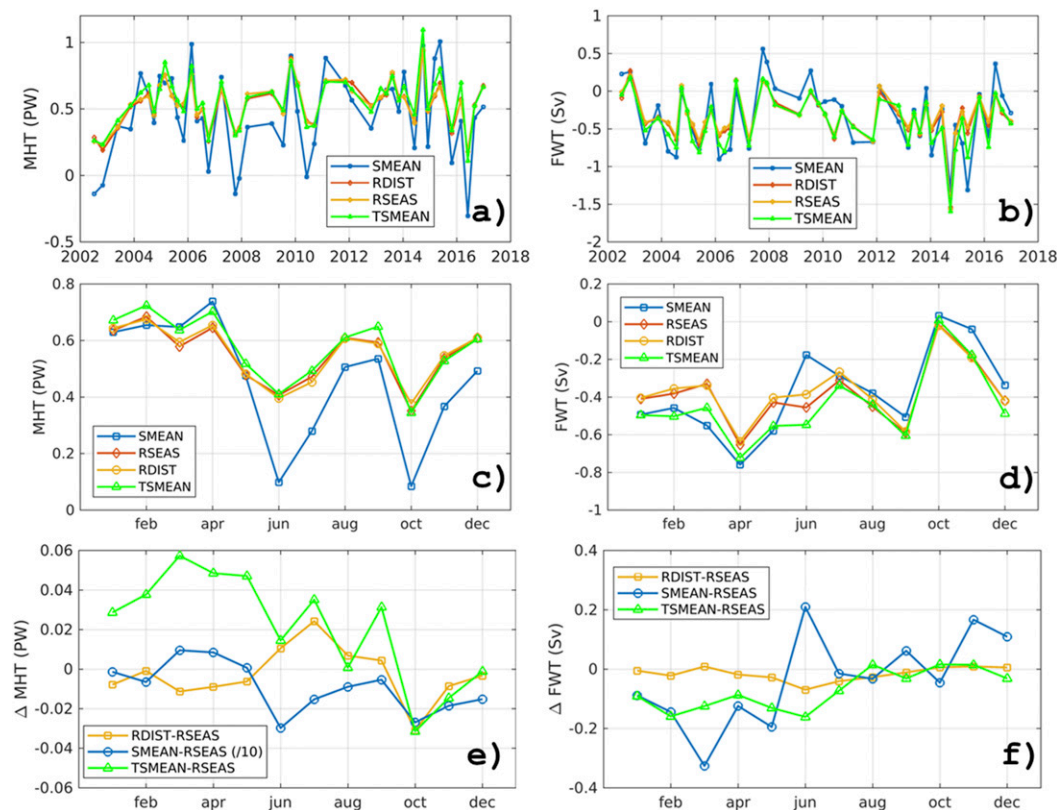


FIG. 8. Estimates of (left) MHT and (right) FWT from the AX18 data using the four salinity estimation methods. (a),(b) Time series using each salinity method; (c),(d) monthly means; and (e),(f) monthly means of residuals relative to RSEAS. The SMEAN-RSEAS residuals in (e) are scaled by 10^{-1} to allow comparison with the other estimates.

XBT observations since 2002 and with satellite altimetry since 1993.

The variability at interannual to decadal time scales is not resolved by the methods presented in this study. In the RSEAS and RDIST methods, some small interannual variability is observed, and accounts for only a ± 0.1 psu in the upper 200 m of the ocean. This variability seems to be related to large-scale processes, such as NAO in the NA and NO, and potentially to ENSO and other large-scale phenomena.

Longer-term salinity trends in the Atlantic have been detected in recent studies (e.g., Durack and Wijffels 2010; Grodsky et al. 2006; Hosoda et al. 2009; Goes et al. 2014). These may be associated with the strengthening of the hydrological cycle (evaporation and precipitation), ocean advection, and are regionally varying. Long-term changes are revealed in the TSMEAN method (Fig. 5), which although subject to coverage biases, they hinge on a freshening at the surface and salinification at central depths in the NA and NO regions. These long-term changes are not observed when the SMEAN method is used, so the trends may

be driven mostly by temperature changes to the mean TS and spiciness instead of salinity itself. These long-term changes and their effect on the distribution of water masses over depth may have large-scale impacts, such as the stability of the AMOC. We tested the sensitivity of the meridional heat and freshwater transports to the empirical salinity estimates across 35°S in the South Atlantic. The sensitivity of the MHT and FWT to different salinity estimates is an order of magnitude smaller than their mean climatological values, and the east and west boundaries are more sensitive to the methodology choice. Although small, the SMEAN method can drive reversals of the MHT and FWT estimates, and is not recommended to be used in the South Atlantic. Other regions such as the North Atlantic may have different impacts, and the TSMEAN method may bring larger errors.

Results of the work presented here have immediate impact on the studies of ocean circulation and climate studies, in particular on studies that use historical and current XBT profile data, and applications for ocean forecast and ocean state estimation, for which salinity plays a critical role. Future improvements for this method

may include 1) large-scale predictors [e.g., NAO, southern annular mode (SAM)], principal component methods of large-scale surface properties, and autoregressive methods, including information about interannual to decadal variability of salinity in the upper ocean, which are only partially represented by the temperature predictors; 2) more structured and variable spatial covariance function, using, for example, weights given from satellite altimetry, and classification methods (clustering), which can efficiently reduce the number of boxes required to define similar T - S patterns (e.g., Maze et al. 2017). This would reduce the noise and mesoscale eddy variability in the mean profile by increasing the number of trial population, particularly in poorly sampled areas; and 3) the methods presented here treat each depth as independent. Assuming depth as an independent variable may bring the advantage of avoiding dealing with depth-varying error variances (heteroscedasticity) and missing data, but loses information of depth autocorrelation. This can be included with depth principal components (e.g., Maes and Behringer 2000) or fitting a structured depth autocovariance matrix (e.g., Goes et al. 2010).

Acknowledgments. This research was accomplished under the auspices of the Cooperative Institute for Marine and Atmospheric Studies (CIMAS), a cooperative institute of the University of Miami and the National Oceanic and Atmospheric Administration (NOAA), Cooperative Agreement NA15OAR4320064, and was partly funded by the Ocean Observing and Monitoring Division of the NOAA Climate Program Office, the NOAA Atlantic Oceanographic and Meteorological Laboratory (AOML), and the National Science Foundation Grant 1537769. The data used in this study are available online: CORA v.3.4 data (www.coriolis.eu.org), AX18 transect data (www.aoml.noaa.gov/phod/hdenxbt/ax_home.php?ax=18), and WOA13 climatology (<https://www.nodc.noaa.gov/cgi-bin/OC5/woa13/woa13.pl>). The authors want to thank Claudia Schmid for helping with the Argo profiles data, and the ship companies and ship riders for carrying out the AX18 transect as part of the NOAA/AOML XBT Network project.

REFERENCES

- Ballabrera-Poy, J., B. Moure, E. Garcia-Ladona, A. Turiel, and J. Font, 2009: Linear and non-linear T - S models for the eastern North Atlantic from Argo data: Role of surface salinity observations. *Deep-Sea Res. I*, **56**, 1605–1614, <https://doi.org/10.1016/j.dsr.2009.05.017>.
- Baringer, M. O., and S. L. Garzoli, 2007: Meridional heat transport determined with expendable bathythermographs—Part I: Error estimates from model and hydrographic data. *Deep-Sea Res. I*, **54**, 1390–1401, <https://doi.org/10.1016/j.dsr.2007.03.011>.
- Cabanes, C., and Coauthors, 2013: The CORA dataset: Validation and diagnostics of in-situ ocean temperature and salinity measurements. *Ocean Sci.*, **9**, 1–18, <https://doi.org/10.5194/os-9-1-2013>.
- Carnes, M. R., W. J. Teague, and J. L. Mitchell, 1994: Interference of subsurface structure from field measurable by satellite. *J. Atmos. Oceanic Technol.*, **11**, 551–566, [https://doi.org/10.1175/1520-0426\(1994\)011<0551:IOSTSF>2.0.CO;2](https://doi.org/10.1175/1520-0426(1994)011<0551:IOSTSF>2.0.CO;2).
- Chang, Y.-S., A. Rosati, and S. Zhang, 2011a: A construction of pseudo salinity profiles for the global ocean: Method and evaluation. *J. Geophys. Res.*, **116**, C02002, <https://doi.org/10.1029/2010JC006386>.
- , S. Zhang, and A. Rosati, 2011b: Improvement of salinity representation in an ensemble coupled data assimilation system using pseudo salinity profiles. *Geophys. Res. Lett.*, **38**, L13609, <https://doi.org/10.1029/2011GL048064>.
- Cheng, L., and Coauthors, 2016: XBT science: Assessment of instrumental biases and errors. *Bull. Amer. Meteor. Soc.*, **97**, 924–933, <https://doi.org/10.1175/BAMS-D-15-00031.1>.
- Domingues, R., G. Goni, S. Swart, and S. Dong, 2014: Wind forced variability of the Antarctic Circumpolar Current south of Africa between 1993 and 2010. *J. Geophys. Res. Oceans*, **119**, 1123–1145, <https://doi.org/10.1002/2013JC008908>.
- Dong, S., S. L. Garzoli, M. O. Baringer, C. S. Meinen, and G. J. Goni, 2009: Interannual variations in the Atlantic meridional overturning circulation and its relationship with the net northward heat transport in the South Atlantic. *Geophys. Res. Lett.*, **36**, L20606, <https://doi.org/10.1029/2009GL039356>.
- , —, and —, 2011: The role of interocean exchanges on decadal variations of the meridional heat transport in the South Atlantic. *J. Phys. Oceanogr.*, **41**, 1498–1511, <https://doi.org/10.1175/2011JPO4549.1>.
- Durack, P. J., and S. E. Wijffels, 2010: Fifty-year trends in global ocean salinities and their relationship to broad-scale warming. *J. Climate*, **23**, 4342–4362, <https://doi.org/10.1175/2010JCLI3377.1>.
- Emery, W. J., and A. O'Brien, 1978: Inferring salinity from temperature or depth for dynamic height calculations in the North Pacific. *Atmos.–Ocean*, **16**, 348–366, <https://doi.org/10.1080/07055900.1978.9649042>.
- , and J. S. Dewar, 1982: Mean temperature-salinity, salinity-depth and temperature-depth curves for the North Atlantic and the North Pacific. *Prog. Oceanogr.*, **11**, 219–305, [https://doi.org/10.1016/0079-6611\(82\)90015-5](https://doi.org/10.1016/0079-6611(82)90015-5).
- Fox, D. N., W. J. Teague, C. N. Barron, M. R. Carnes, and C. M. Lee, 2002: The Modular Ocean Data Assimilation System (MODAS). *J. Atmos. Oceanic Technol.*, **19**, 240–252, [https://doi.org/10.1175/1520-0426\(2002\)019<0240:TMODAS>2.0.CO;2](https://doi.org/10.1175/1520-0426(2002)019<0240:TMODAS>2.0.CO;2).
- Garzoli, S., M. Baringer, S. Dong, R. Perez, and Q. Yao, 2013: South Atlantic meridional fluxes. *Deep-Sea Res. I*, **71**, 21–32, <https://doi.org/10.1016/j.dsr.2012.09.003>.
- Goes, M., N. M. Urban, R. Tonkonojekov, M. Haran, A. Schmittner, and K. Keller, 2010: What is the skill of ocean tracers in reducing uncertainties about ocean diapycnal mixing and projections of the Atlantic Meridional Overturning Circulation? *J. Geophys. Res.*, **115**, C12006, <https://doi.org/10.1029/2010JC006407>.
- , G. Goni, V. Hormann, and R. Perez, 2013: Variability of the Atlantic off-equatorial eastward currents during 1993–2010 using a synthetic method. *J. Geophys. Res. Oceans*, **118**, 3026–3045, <https://doi.org/10.1002/jgrc.20186>.
- , I. Wainer, and N. Signorelli, 2014: Investigation of the causes of historical changes in the subsurface salinity minimum of

- the South Atlantic. *J. Geophys. Res. Oceans*, **119**, 5654–5675, <https://doi.org/10.1002/2014JC009812>.
- , G. Goni, and S. Dong, 2015a: An optimal XBT-based monitoring system for the South Atlantic meridional overturning circulation at 34°S. *J. Geophys. Res. Oceans*, **120**, 161–181, <https://doi.org/10.1002/2014JC010202>.
- , M. Baringer, and G. Goni, 2015b: The impact of historical biases on the XBT-derived meridional overturning circulation estimates at 34°S. *Geophys. Res. Lett.*, **42**, 1848–1855, <https://doi.org/10.1002/2014GL061802>.
- Goni, G. J., and Coauthors, 2010: The Ship of Opportunity Program. *Proceedings of OceanObs'09: Sustained Ocean Observations and Information for Society*, J. Hall, D. E. Harrison, and D. Stammer, Eds., Vol. 2, ESA Publ. WPP-306, <https://doi.org/10.5270/OceanObs09.cwp.35>.
- Grodsky, S. A., J. A. Carton, and F. M. Bingham, 2006: Low-frequency variation of sea surface salinity in the tropical Atlantic. *Geophys. Res. Lett.*, **33**, L14604, <https://doi.org/10.1029/2006GL026426>.
- Guinehut, S., A.-L. Dhomps, G. Larnicol, and P.-Y. Le Traon, 2012: High resolution 3-D temperature and salinity fields derived from in situ and satellite observations. *Ocean Sci.*, **8**, 845–857, <https://doi.org/10.5194/os-8-845-2012>.
- Haines, K., J. D. Blower, J.-P. Drecourt, C. Liu, A. Vidard, I. Astin, and X. Zhou, 2006: Salinity assimilation using $S(T)$: Covariance relationships. *Mon. Wea. Rev.*, **134**, 759–771, <https://doi.org/10.1175/MWR3089.1>.
- Hansen, D. V., and W. C. Thacker, 1999: Estimation of salinity profiles in the upper ocean. *J. Geophys. Res.*, **104**, 7921–7933, <https://doi.org/10.1029/1999JC900015>.
- Hosoda, S., T. Sugo, N. Shikama, and K. Mizuno, 2009: Global surface layer salinity change detected by Argo and its implication for hydrological cycle intensification. *J. Oceanogr.*, **65**, 579–586, <https://doi.org/10.1007/s10872-009-0049-1>.
- Huang, B., Y. Xue, and D. W. Behringer, 2008: Impacts of Argo salinity in NCEP Global Ocean Data Assimilation System: The tropical Indian Ocean. *J. Geophys. Res.*, **113**, C08002, <https://doi.org/10.1029/2007JC004388>.
- Korotenko, K. A., 2007: A regression method for estimating salinity in the ocean. *Oceanology*, **47**, 464–475, <https://doi.org/10.1134/S0001437007040030>.
- Lima, M., M. Cirano, M. Mata, M. Goes, G. Goni, and M. O. Baringer, 2016: An assessment of the Brazil Current baroclinic structure and variability near 22°S in distinct Ocean Forecasting and Analysis Systems. *Ocean Dyn.*, **66**, 893, <https://doi.org/10.1007/s10236-016-0959-6>.
- Locarnini, R. A., and Coauthors, 2013: *Temperature*. Vol. 1, *World Ocean Atlas 2013*, NOAA Atlas NESDIS 73, 40 pp.
- Machín, F., M. Emelianov, P. Rodríguez, E. García-Ladona, J. Menéndez, and J. Salat, 2008: XBT profilers for operational purposes: Application and validation in real exercises. *Sci. Mar.*, **72**, 779–799, <https://doi.org/10.3989/scimar.2008.72n4779>.
- Maes, C., and D. Behringer, 2000: Using satellite-derived sea level and temperature profiles for determining the salinity variability: A new approach. *J. Geophys. Res.*, **105**, 8537–8547, <https://doi.org/10.1029/1999JC900279>.
- Marrero-Díaz, A., A. Rodríguez-Santana, F. Machín, and J. L. Pelegrí, 2006: Analytic salinity-temperature relations for the upper-thermocline waters of the eastern North Atlantic subtropical gyre. *Sci. Mar.*, **70**, 167–175, <https://doi.org/10.3989/scimar.2006.70n2167>.
- Maze, G., H. Mercier, R. Fablet, P. Tandeo, M. L. Radenco, P. Lenca, C. Feucher, and C. Le Goff, 2017: Coherent heat patterns revealed by unsupervised classification of Argo temperature profiles in the North Atlantic Ocean. *Prog. Oceanogr.*, **151**, 275–292, <https://doi.org/10.1016/j.pocean.2016.12.008>.
- Reseghetti, F., 2007: Empirical reconstruction of salinity from temperature profiles with phenomenological constraints. *Ocean Sci. Discuss.*, **4**, 1–39, <https://doi.org/10.5194/osd-4-1-2007>.
- Reverdin, G., F. Durand, J. Mortensen, F. Schott, H. Valdimarsson, and W. Zenk, 2002: Recent changes in the surface salinity of the North Atlantic subpolar gyre. *J. Geophys. Res.*, **107**, 8010, <https://doi.org/10.1029/2001JC001010>.
- Ridgway, K. R., J. R. Dunn, and J. L. Wilkin, 2002: Ocean interpolation by four-dimensional weighted least squares—Application to the waters around Australasia. *J. Atmos. Oceanic Technol.*, **19**, 1357–1375, [https://doi.org/10.1175/1520-0426\(2002\)019<1357:OIBFDW>2.0.CO;2](https://doi.org/10.1175/1520-0426(2002)019<1357:OIBFDW>2.0.CO;2).
- Smith, G. C., and K. Haines, 2009: Evaluation of the $S(T)$ assimilation method with the Argo dataset. *Quart. J. Roy. Meteor. Soc.*, **135**, 739–756, <https://doi.org/10.1002/qj.395>.
- Stommel, H., 1947: Note on the use of the T-S correlation for dynamic height anomaly computations. *J. Mar. Res.*, **6**, 85–92.
- Sverdrup, H. U., M. W. Johnson, and R. H. Fleming, 1942: *The Oceans: Their Physics, Chemistry, and General Biology*. Prentice-Hall, 1087 pp.
- Thacker, W. C., 2007: Estimating salinity to complement observed temperature: 1. Gulf of Mexico. *J. Mar. Syst.*, **65**, 224–248, <https://doi.org/10.1016/j.jmarsys.2005.06.008>.
- , 2008: Estimating salinity between 25° and 45°S in the Atlantic Ocean using local regression. *J. Atmos. Oceanic Technol.*, **25**, 114–130, <https://doi.org/10.1175/2007JTECHO530.1>.
- van Caspel, M. R., M. Magalhães Mauricio, and M. Cirano, 2010: On the TS relationship in the central region of the Southwest Atlantic: A contribution for the study of ocean variability in the vicinity of the Vitória-Trindade chain. *Atlântica*, **32**, 95–110, <https://doi.org/10.5088/atlantica.v32i1.1556>.
- Yang, T., Z. Chen, and Y. He, 2015: A new method to retrieve salinity profiles from sea surface salinity observed by SMOS satellite. *Acta Oceanol. Sin.*, **34** (9), 85–93, <https://doi.org/10.1007/s13131-015-0735-3>.
- Zweng, M. M., and Coauthors, 2013: *Salinity*. Vol. 2, *World Ocean Atlas 2013*, NOAA Atlas NESDIS 74, 39 pp.